ACS Catalysis

Research Article

Cite This: ACS Catal. 2018, 8, 11352−11361

pubs.acs.org/acscatalysis

How Proximal Nucleobases Regulate the Catalytic Activity of G-Quadruplex/Hemin DNAzymes

Jielin Chen,[†] Yingying Zhang,[†] Mingpan Cheng,[†] Yuehua Guo,[†] Jiri Šponer,[‡] David Monchaud,[§] Jean-Louis Mergny,[†,‡,∥] Huangxian Ju,*[,†] and Jun Zhou*[,†]

[†]State Key Laboratory of Analytical Chemistry for Life Science, School of Chemistry and Chemical Engineering, Nanjing University, Nanjing 210023, China

[‡]Institute of Biophysics of the Czech Academy of Sciences, Královopolská 135, 612 65 Brno, Czech Republic

[§]Institut de Chimie Moléculaire (ICMUB), CNRS UMR6302, UBFC Dijon 21078, France

[∥]Université de Bordeaux, INSERM U1212, CNRS UMR 5320, ARNA Laboratory, IECB, 33600 Pessac, France

Supporting Information

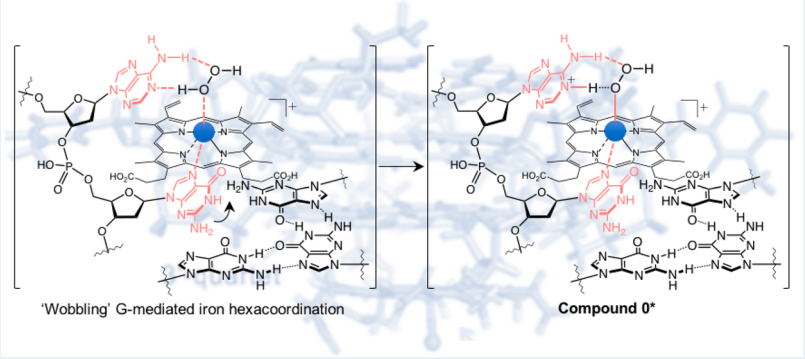

ABSTRACT: G-quadruplexes (G4s) are versatile catalytic DNAs when combined with hemin. Despite the repertoire of catalytically competent G4/hemin complexes studied so far, little is known about the detailed catalytic mechanism of these biocatalysts. Herein, we have carried out an in-depth analysis of the hemin binding site within the G4/hemin catalysts, providing the porphyrinic cofactor with a controlled nucleotidic environment. We intensively assessed the position-dependent catalytic enhancement in model reactions and found that proximal nucleobases enhance the catalytic ability of the G4/hemin complexes. Our results allow for revisiting the mechanism of the G4/hemin-based catalysis, especially gaining insights into the rate-limiting step, demonstrating how both the G4 core and the proximal nucleotides dA and/or dC concomitantly activate the Compound 0 → 0* prototropic cleavage of H_2O_2 to foster Compound 1 formation. These results provide mechanistic clues as to how the properties of G4-based catalysts can be improved to ultimately make them competitive with proteinaceous enzymes.

KEYWORDS: *DNAzyme, G4/hemin complex, G4-based catalyst, G-quartet, proximal nucleobases*

INTRODUCTION

Although most biocatalysts are protein enzymes[1] and RNAs (ribozymes),[2−4] biomolecular catalysis can also be achieved by synthetic genetic polymers[5] and DNA.[6−8] DNAzymes, discovered in 1994 by Breaker and Joyce,[9] have been exploited to catalyze a wide variety of chemical transformations including DNA/RNA ligation,[10,11] DNA photorepair,[12,13] and organic synthesis reactions[14] including Michael additions,[15−17] Diels−Alder reactions,[18,19] and oxidation of organic substrates.[6,20,21]

One of the best-characterized DNAzymes is the G-quadruplex (G4)/hemin peroxidase-mimicking DNAzyme, which has been extensively exploited as a promising candidate for various applications.[22−24] This system is formed by the association of relatively short, guanine-rich oligonucleotides that can fold into four-stranded G4 structures and Fe(III)-protoporphyrin IX (hemin), the cofactor of many natural oxidases (horseradish peroxidase, HRP, among others).[25] The G4 structure provides a binding pocket for hemin, which nestles in between the accessible G-quartet of the G4 and the surrounding nucleobases. However, the exact properties of this active site remain elusive, as do the fine mechanistic details that govern the overall catalytic activity of the G4/hemin system.

G4/hemin DNAzymes have been used to promote the H_2O_2-mediated oxidation of many substrates including 2,2′-azino-bis(3-ethylbenzothiozoline-6-sulfonic acid) (ABTS),[26] luminol,[27] β-nicotinamide adenine dinucleotide (NADH),[28] dopamine,[29] among others.[30−32] The wealth of data acquired over the past few years have confirmed that G4/hemin

Received: September 21, 2018
Revised: October 19, 2018
Published: October 24, 2018

DOI: 10.1021/acscatal.8b03811
ACS Catal. 2018, 8, 11352−11361

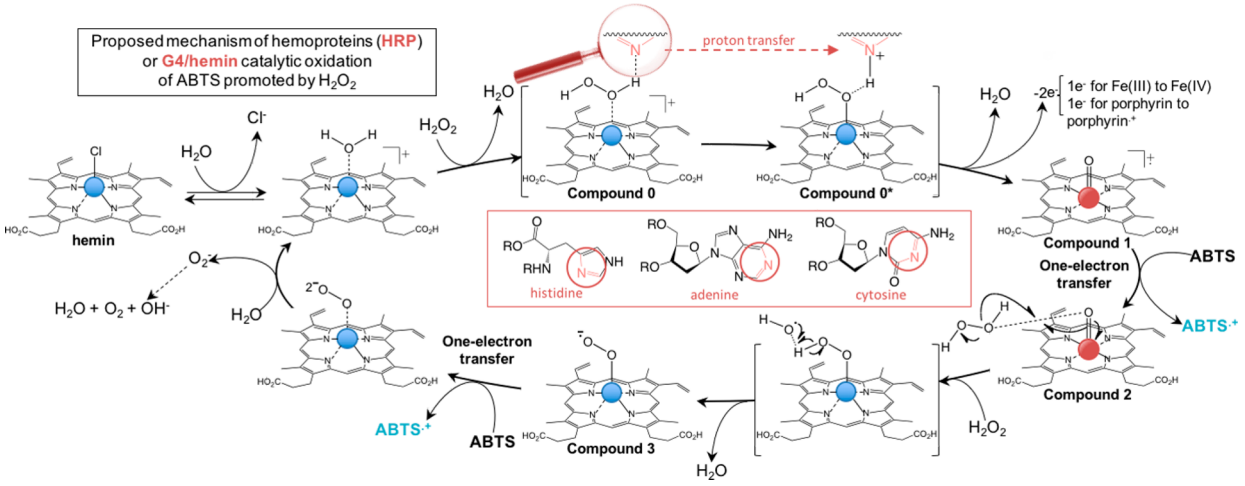

Figure 1. Proposed mechanism of ABTS oxidation catalyzed by either the proteinaceous HRP or the G4-based DNAzymes. Highlighted are the histidine and nucleobases in the hemin binding sites of HRP and the DNAzyme that act as H_2O_2 activators via proton transfer. Blue spheres represent Fe(III), and red spheres denote Fe(IV).

DNAzymes are versatile biocatalysts but also revealed that the catalytic efficiency of DNAzymes is still low compared with that of native, proteinaceous enzymes. Therefore, various strategies to improve this efficacy have been recently developed and successfully attempted.[33−37] For example, efforts have been invested to decipher the relationship between the G4 topology and its catalytic activity, highlighting the overall better performances of the parallel G4/hemin DNAzymes.[33] Exogenous agents, such as adenosine triphosphate (ATP),[34,35] DOTASQ[36] and spermine,[37] have also been described as efficient additives to boost the G4-based catalysis. We and others also revealed that the catalytic activity can be enhanced by modulating the flanking and/or loop sequences of parallel G4s.[38−40] However, insights into the exact nature of the hemin binding pocket within the G4 structure, which can affect the rate-limiting step of G4/hemin DNAzyme, are still urgently needed. Here, we interrogated how proximal nucleotides in the G4 loops and flanking regions influence the catalysis, with the hope of recreating enzyme-like hemin environment.

In the HRP active site, a histidine (His42) actively participates in the catalysis by promoting the prototropic isomerization of H_2O_2 once bound to the hemin iron atom, and intervenes in the formation of both the first (Compound 0) and second catalytic intermediate (Compound 0*) via a proton transfer step.[41] When applied to G4-based DNAzyme, a nine-step catalytic cycle can be proposed (Figure 1) in which an adenine (dA) or a cytosine (dC) nucleotide near the hemin binding site might activate the Compound 0 → 0* proton transfer in a histidine-like manner.[34] To assess the relevance of this catalytic mechanism, we systematically varied here the lengths and sequences in the G4 loops and flanking regions to investigate whether and to which extent proximal nucleotides influence the catalytic efficiency of the resulting DNAzymes. Our data demonstrate that an optimally located nucleobase in the vicinity of the G-quartet indeed activates the Compound 0 → 0* proton transfer in a His42-like manner. Our investigations also provide fundamental insights into how to design new-generation DNAzymes.

MATERIALS AND METHODS

Materials and Reagents. PAGE or HPLC purified oligonucleotides were purchased from Sangon Biotech (Shanghai, China) without further purification. They were dissolved in ultrapure water (18.2 MΩ·cm) and used without further purification. Their concentrations were determined by UV absorbance at 260 nm using the molar extinction coefficients provided by OligoAnalyzer 3.1 (http://sg.idtdna.com/calc/analyzer). To fold G-quadruplexes, the DNA samples were heated to 95 °C for 5 min, cooled slowly to room temperature, and then stored at 4 °C overnight or longer before use.

Hemin was dissolved in DMSO and diluted to 0.1 mM and then stored in the dark at 4 °C. Freshly prepared ABTS and NADH were dissolved in ultrapure water to 50 mM, and TMB was dissolved in DMSO to 50 mM. Except for analysis of pH effects, all experiments were performed in 10 mM Tris-HCl (pH 7.0) containing 0.05% Triton X-100, 1% DMSO, and 100 mM KCl. All the chemicals were obtained from Sigma.

G4 DNAzyme Activity Measurements. The annealed G4s (0.4 μM) diluted from the corresponding stock solutions were incubated with hemin (0.8 μM) in 10 mM Tris-HCl (pH 7.0) containing 0.05% Triton X-100, 1% DMSO, and 100 mM KCl for 2 h at 25 °C. After the formation of G4/hemin complexes, the substrate (ABTS, TMB, or NADH at a final concentration of 0.6 mM) and H_2O_2 (0.6 mM) were added. Product formation was followed by monitoring the absorbance of $ABTS^{\cdot+}$ at 420 nm, $TMB^{\cdot+}$ at 652 nm, and NADH at 340 nm using a Cary100 (Agilent) spectrophotometer for 60 s using extinction coefficients of 36 000 M^{-1} cm^{-1} for $ABTS^{\cdot+}$ at 420 nm (Figure S1), 39 000 M^{-1} cm^{-1} for $TMB^{\cdot+}$ at 652 nm (Figure S2), and 6220 M^{-1} cm^{-1} for NADH at 340 nm (Figure S3). The initial rate (V_0, nM/s) of the oxidation reaction was obtained from the slope of the initial linear portion (the first 10 s) of the plot of absorbance versus reaction time. All kinetic measurements were repeated three times, and the background activity of hemin alone was subtracted.

Circular Dichroism (CD) Measurements. CD spectra were collected on a Chirascan circular spectropolarimeter (Applied Photophysics) in the 220−350 nm wavelength range. G4 solutions (5 μM strand concentration) were obtained by directly diluting the stock solutions of DNAs (10 μM) into 10 mM Tris-HCl buffer containing 100 mM KCl (pH 7.0). The lamp was kept under a stable stream of dry purified nitrogen

DOI: 10.1021/acscatal.8b03811
ACS Catal. 2018, 8, 11352−11361

(99.99%) during experiments, and the measurements were repeated three times.

Spectroscopic Characterization of Peroxidation Intermediate. G4s (1 μM) were incubated with hemin (2 μM) in 10 mM Tris-HCl (pH 7.0), 1% DMSO, and 0.05% Triton X-100 at 25 °C for 2 h. To evaluate the decay kinetics of the G4/hemin complexes, H_2O_2 (0.4 mM) was added, and absorbance at 404 nm was monitored over time. The initial degradation velocity was obtained from the slope of the initial linear portion (the first 5 s) in the plot of absorbance versus reaction time. To monitor generation of Compound 1, experiments were conducted in the presence of 10 μM DNA, 10 μM hemin, and 0.75 mM H_2O_2 in 10 mM Tris-HCl (pH 7.0) containing 1% DMSO, and 0.05% Triton X-100, and spectra were collected from 450 to 700 nm as a function of time.

pH Dependence of G-Quadruplex DNAzyme Activity. pH dependence experiments were conducted in 20 mM Britton-Robinson buffers solution (pH 2.83−7.08). (Note: to avoid buffer composition effects, we kept the same buffer.) All buffer solutions contained 20 mM acetic acid, 20 mM orthophosphoric acid, 20 mM boric acid, 100 mM KCl, 1% DMSO, and 0.05% Triton X-100. G4s (0.4 μM) were incubated with 0.8 μM hemin at 25 °C for 2 h, and 0.6 mM ABTS and 0.6 mM H_2O_2 were added to initiate the reaction. The reactions were monitored by UV−vis absorbance on a Cary100 (Agilent) spectrophotometer, and data were converted to reaction rate (V_0 values, nM/s) as described above. All measurements were repeated three times, and background reactions (that is, reactions performed without G4s) were subtracted.

Dissociation Constant (K_d) Determination. To evaluate the affinity between G4s and hemin, a spectrophotometric titration of hemin with increasing concentrations of DNA was performed by incubating G4 (0 to 10 μM) with hemin (5.0 μM) in 10 mM Tris-HCl buffer at 25 °C for 2 h. Spectra were collected from 350 to 600 nm. The saturation curves for the binding of hemin with G4s were determined by plotting fraction of bound hemin (α, determined by eq 1) as a function of DNA concentration and fitting with a one-site binding model, using GraphPad Prism 5, to extract K_d values for every sequence. K_a was defined as the reciprocal of K_d on the basis of K_a*K_d = 1. eq 1 is

$$\alpha = \frac{A_x - A_0}{A_\infty - A_0} \quad (1)$$

where A_x is the absorbance at 404 nm for DNA incubated with hemin, A_∞ and A_0 are the respective values in the presence of saturating DNA and in the absence of DNA, respectively.

RESULTS AND DISCUSSION

Catalytic Activity of Nonparallel G-Quadruplex/Hemin DNAzyme. Recent works suggested that either a single dA or dA/dC runs near the external G-quartet of parallel G4s can enhance the catalytic ability of G4/hemin biocatalysts.[38−40] In these investigations, G4 topologies were restricted to parallel structures. To assess whether nonparallel topologies behave similarly, we designed a series of hybrid G4s with the sequence d[$AG_3(T_2AG_3)_3T_nM$] where M is a dA or dC nucleotide (Series I, Table 1), introduced at or near the 3′-terminal G-quartet of the G4/hemin catalyst (see the schematic representation in Figure S4). Circular dichroism (CD) investigations (Figure S5A and Table S1) confirmed the hybrid-type topology of the resulting G4 architectures in K^+-containing buffer.[42] When compared with the parent, non-modified sequence H1, we found that although a single dA or dC enhanced the catalytic activity in a position-dependent manner, its effect was poorly significant (Figure S5B). We then evaluated DNAzymes with dAs in either the first or second G4 loop (i.e., d[$AG_3A_nG_3(T_2AG_3)_2$] and d-[$AG_3T_2AG_3A_nG_3T_2AG_3$], AnL1-H1 and AnL2-H1, respectively; Series II, Table 1): these DNAzymes adopted a hybrid-type topology (Figure S5C) and displayed better activity than the parent H1 (For example, A7L2-H1, 4.9-fold enhancement, Figure S5D). However, this strategy relied on nonparallel G4s thus suffering from topological dynamism and structural polymorphism (as indicated by CD studies, Figure S5C), thereby obscuring the actual origins of the changes in catalytic competencies. To tackle this issue, we decided to work

Table 1. Tested Oligonucleotides in this Work

Name	Sequences (5'-3')
Parent sequences of non-parallel and parallel form DNAzymes	
H1	AGGGTTAGGGTTAGGGTTAGGG
G3T	GGGTGGGTGGGTGGG
Reference sequences [a]	
LA4	GGGTGGGAAAAGGGTGGG
LA (or AT_0, T_0A-G4)	GGGTGGGAGGGTGGG
LC (or CT_0, T_0C-G4)	GGGTGGGCGGGTGGG
LT12	GGGTGGGTTTTTTTTTTTTGGGTGGG
(I) Non-parallel G-quadruplexes with different flanking sequences (n = 0, 1, 2)	
H1-TnA	AGGGTTAGGGTTAGGGTTAGGGT_nA
H1-TnC	AGGGTTAGGGTTAGGGTTAGGGT_nC
(II) Non-parallel G-quadruplexes with different loops (n = 1, 3, 5, 7)	
AnL1-H1	AGGGA_nGGGTTAGGGTTAGGG
AnL2-H1	AGGGTTAGGGA_nGGGTTAGGG
(III) Parallel G-quadruplexes with different loops (n = 1, 2, 3, 4, 5, 8, 11)	
AT_n-G4	GGGTGGGAT_nGGGTGGG
T_nA-G4	GGGTGGGT_nAGGGTGGG
CT_n-G4	GGGTGGGCT_nGGGTGGG
T_nC-G4	GGGTGGGT_nCGGGTGGG
(IV) Parallel G-quadruplexes with the same loop length (n = 0, 1, 2, 3, ...10, 11)	
T_nAT_{11-n}G4	GGGTGGGT_nAT_{11-n}GGGTGGG
(V) Parallel G-quadruplexes with d[TC] or d[CT] in different length loops (n = 1, 2, 3, 4, 5, 6, 9, 12, 14, 16)	
TCT_n-G4	GGGTGGGTCT_nGGGTGGG
T_nCT-G4	GGGTGGGT_nCTGGGTGGG
(VI) Parallel G-quadruplexes with different flanking sequences (n = 0, 1, 2)	
F5T_nA	AT_nGGGTGGGTGGGTGGG
F3T_nA	GGGTGGGTGGGTGGGT_nA
F5T_nC	CT_nGGGTGGGTGGGTGGG
F3T_nC	GGGTGGGTGGGTGGGT_nC
F5C3	CCCGGGTGGGTGGGTGGG
F3C3	GGGTGGGTGGGTGGGCCC
FC3	CCCGGGTGGGTGGGTGGGCCC
(VII) Parallel G-quadruplexes with different alkyl chains (lowercase letter n means the number of methylenes in alkyl chain, n = 3, 6, 12)	
LAMet$_n$	GGGTGGGA $(CH_2)_n$GGGTGGG
FMet$_n$A	GGGTGGGTGGGTGGG$(CH_2)_n$ A
FMet$_n$C	GGGTGGGTGGGTGGG$(CH_2)_n$ C
(VIII) Parallel G-quadruplexes with a tail (underlined) in 3'-terminal	
G4-T	TTGGGTGGGTGGGTGGGTTTTTTCATCTAGGC
(IX) Single strand complementary with underlined tail sequence in VIII	
18t	GCC TAG ATG AAA AAA TTC
17t	GCC TAG ATG AAA AAA TC
16t	GCC TAG ATG AAA AAA C
15t	GCC TAG ATG AAA AA C
14t	GCC TAG ATG AAA A C
13t	GCC TAG ATG AAA C

[a] LA4 was introduced in our previous work,[38] and used here as reference because of its excellent activation.

DOI: 10.1021/acscatal.8b03811
ACS Catal. 2018, 8, 11352−11361

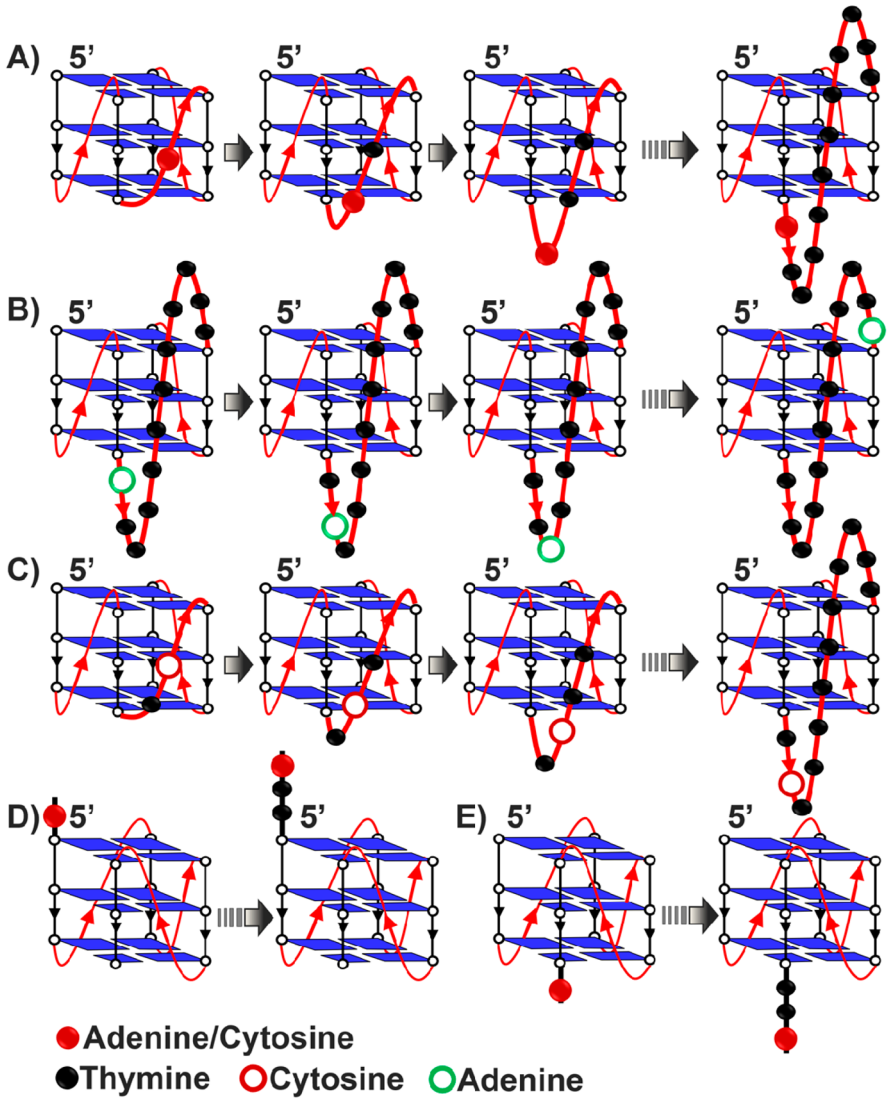

Figure 2. Schematic representations of parallel G4 structures investigated in this study. Each motif has two single-nucleotide loops that constrain the fold into a parallel conformation. We tested G4s with (A) dA- or dC-containing (indicated by red balls) loops of different lengths (Series III in Table 1), (B) a 12-nucleotide loop with dA in different locations (Series IV), (C) a loop with dC in different locations in a variable length loop (Series V), (D) dC in the 5′ flanking sequence (Series VI), and (E) dC in the 3′ flanking sequence (Series VI). See Figure S4 for schemes of nonparallel G4 forms.

exclusively with parallel G4s in all subsequent investigations (schematics shown in Figure 2).

Peroxidative Behavior of Parallel G-Quadruplex/Hemin DNAzyme. *Influence of Proximal Nucleobases in the Second Loop of Parallel G4 DNAzymes.* A recent report suggested that parallel or hybrid G4s offer more proficient hemin binding sites than antiparallel G4s because the loops of antiparallel G4s partially obstruct hemin cofactor interact with G-quartet and may also shield the hemin, resulting in reduced accessibility of hemin to the substrates.[43] However, as indicated above, hybrid G4s also suffered from a conformational plurality that precludes in-depth mechanistic investigations. We thus wondered whether the catalytic activity of parallel G4s, known for their structural unicity and robustness, might be optimized and fine-tuned by proximal dA/dC modifications.

To test this hypothesis, we used sequences with two single-nucleotide loops, known to adopt parallel conformations,[44] and systematically modified the second loop with different loop lengths and dA locations, either near the 3′- or 5′-quartet of G4s (Series III, Table 1; Figure 2A). CD investigations confirmed the parallel conformations of all G4s, with characteristic positive peaks around 260 nm and negative peaks around 240 nm (Figures S6A,B). We found that DNAzyme activity of parallel G4s was dependent on the position of the dA modifications, being fine-tuned by the different number of thymines, with better results obtained when dA was present near the 3′-terminal G-quartet of the G4 (Figure 3A) and with longer loops (for instance, the initial velocity V_0 increased from 30.4 to 183.4 nM/s, when the loop sequences of G4 changed from d[AT_0] to d[AT_3]). Interestingly, the system with a d[AT_3] loop had activity comparable to that with a d[A_4] loop (reference sequence LA4,

DOI: 10.1021/acscatal.8b03811
ACS Catal. 2018, 8, 11352−11361

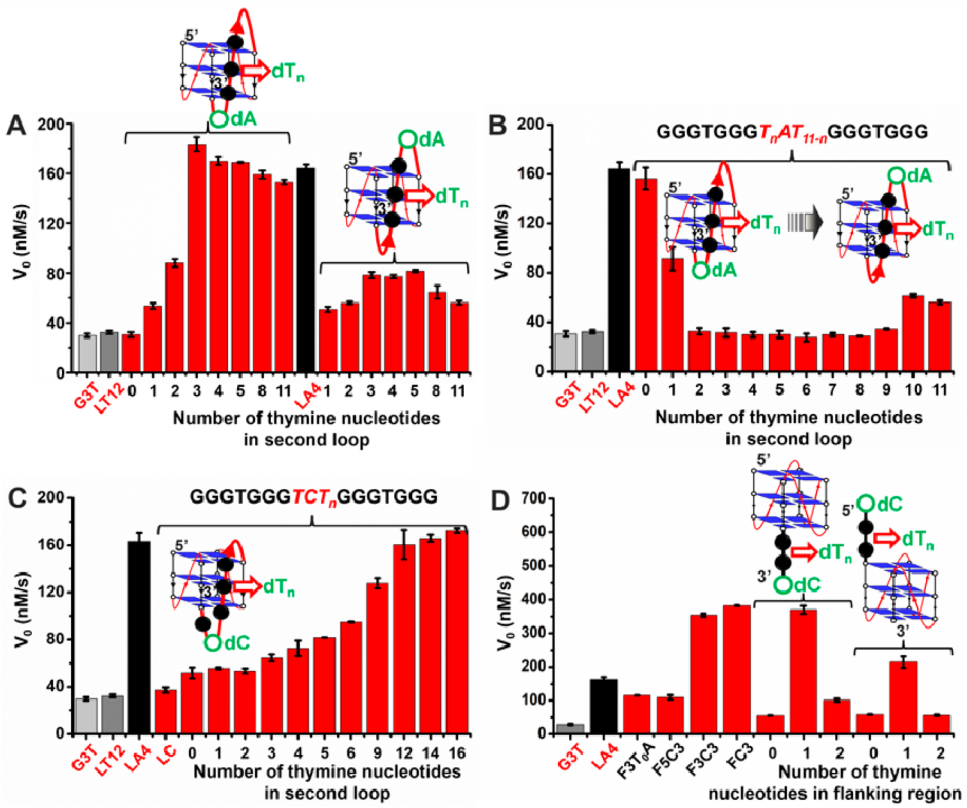

Figure 3. DNAzyme activity (V_0, expressed as nM/s) of parallel G-quadruplexes with (A) different loop lengths and dA located near the 3′ or 5′ G-quartet of the G4, (B) 12-nucleotide loops with dA shifted from the 3′ to 5′ G-quartet, (C) different loop lengths with d[TC] located near the 3′ end, and (D) either d[C_3] or dC arranged as flanking sequences at the 5′ or the 3′ end or both.

V_0 = 164.4 nM/s, which was the best sequence when we investigated the nucleotide repeats on the G4/hemin DNAzyme activity),[38] highlighting that a single dA was sufficient to provide active G4-based catalysts. Lengthening loops to more than four nucleotides had little effect on the catalytic activity of DNAzyme systems (Figure 3A), possibly because longer loops might also influence the stability of the G4s. When a single dA modification was introduced near the 5′-terminal G-quartet (Series III, Table 1), a modest enhancement of the catalytic activity (~2-fold) was found, independently of the number of dT residues (Figure 3A). These data indicated that the modifications near the 3′-terminal G-quartet have more impact on the catalysis than those near the 5′-terminal G-quartet, in agreement with the previously demonstrated preferential binding of hemin to the 3′ G-quartet.[39]

To further characterize the hemin binding site, we decided to eliminate possible loop-length effects, studying parallel G4s with 12-nucleotide loops (Series IV, Table 1), changing only the position of the dA from the 3′- to the 5′-terminal quartet in a stepwise manner (Figure 2B, the formation of parallel structures was confirmed by CD, Figure S7). Collected results demonstrated that dA activates the catalysis only when located at loop ends (the efficiency decreasing with dA located far from the G-quartet, with V_0 = 156.4 and 32.6 nM/s for d[AT_{11}] and d[T_2AT_9], respectively), with a more pronounced effect near the 3′-terminal G-quartet (Figure 3B). These results indicated that the dA-mediated activity enhancement is reliant on the appropriate position of dA relative to the hemin binding site within the G4 structure.

We next assessed the influence of dC modifications following a similar methodology. In this series, single dC modifications were introduced near the 3′- or 5′-terminal G-quartets of the G4s (Series III, Table 1). The formation of parallel structures was confirmed by CD (Figures S6C,D). The slight catalytic enhancements relative to the G4 with an all dT loop (LT12) were insensitive to the position of dC (Figure S8A). To further investigate this, we reasoned that the differences between DNAzymes with dA versus dC in the second loop might originate from either steric or electronic effects, or both: indeed, dA is not only larger (purine ring vs pyrimidine ring) but also electron-richer than dC (due to the proximal carbonyl group in dC, Figure 1). If steric effects underlie the dA/dC difference, a way to improve the activity of dC-containing DNAzymes is to provide dC with more flexibility. We thus studied parallel G4s with d[TCT_n] and d[T_nCT] loops (Series V, Table 1; Figure 2C): enhancements relative to LT12 were modest when dC was near the 3′-terminal G-quartet of the G4, but remarkable when the loop sequence was changed from d[TCT_4] to d[TCT_{12}] (V_0 enhanced from 72.6 to 160.5 nM/s), in a manner that is dependent on loop length and tended to a plateau with longer sequences (Figures 3C and S9). Surprisingly, little terminal selectivity was found, since a similar trend was observed when the dC modification was near the 5′-terminal G-quartet (Figure S8B). It is noteworthy that single dC modifications lead to the same level of catalytic enhancement as dA modifications: for instance, G4s with d[AT_3] and d[TCT_{16}] loops had comparable catalytic activities (V_0 values of 183.4 nM/s and 172.2 nM/s, respectively), despite significant sequence differences.

DOI: 10.1021/acscatal.8b03811
ACS Catal. 2018, 8, 11352−11361

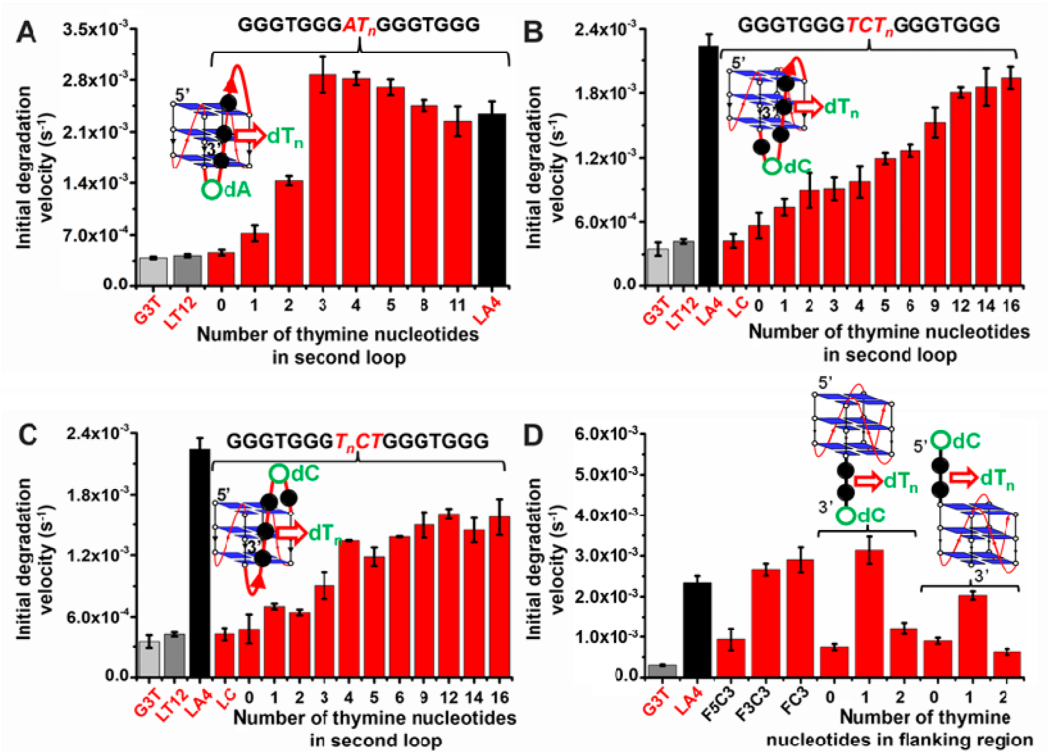

Figure 4. Decay kinetics of G-quadruplex/hemin in the presence of H_2O_2 monitored by absorbance at 404 nm with G4 bearing (A) dA in the second loop, (B) d[TC] near the 3′ end of the second loop, (C) d[CT] near the 5′ end of the second loop, and (D) dC in the flanking sequences.

Influence of Proximal Nucleobases in the Flanking Sequences of Parallel G4 DNAzymes. To further investigate the effect of a single dC on catalytic enhancement, we designed a series of parallel G4 structures in which d[C_3] runs were located at either the 3′ or 5′ end, or both, and G4s in which the dC was separated from the terminal G-quartet by one dT or more (Series VI, Table 1; Figures 2D, 2E and S10). The presence of a d[C_3] tract at 3′ or 5′ end enhanced the activity (V_0 = 353.9 and 109.2 nM/s for F3C3 and F5C3, respectively). Having just a single dC overhang had little effect, but a d[TC] flanking sequence at the 3′ end showed excellent activity (V_0 = 369.9 nM/s, 12-fold vs G3T), comparable to the G4 with d[C_3] at the 3′ or both terminus (Figure 3D). Interestingly, when more dTs were inserted between the dC and the external G-quartet, the activity decreased. We performed similar investigations with dA (Series VI, Table 1; results shown in Figure S11), finding that a direct connection of dA to the 3′ G-quartet was not optimal. Importantly, dC enhanced DNAzyme activity to a greater extent than dA.

Further Insights into the Role Played by Adenine or Cytosine Proximal to G4 Core. We confirmed the generality of the dA/dC-based enhancement of the catalysis through the oxidation of two other substrates, 3,3′,5,5′-tetramethylbenzidine (TMB) and NADH (Figures S12 and S13). We also demonstrated that only the dA/dC position matters, through a series of G4s in which an alkyl linker, $(Met)_n$, was introduced as a spacer between the single dA/dC and the terminal G-quartet (Series VII, Table 1): we demonstrated not only that alkyl linkers do not preclude G4 formation (Figure S14) but also that the resulting G4s behave similarly to those in which the distance between dA/dC and the G-quartet is regulated by dT. The catalytic activity was found to depend on the length of the dA-containing loops (the longer, the better, with V_0 values from 35.7 to 217.2 nM/s when the linker length was increased from Met_0 to Met_{12}, Figure S15A). However, it was essential to separate the dC from the G-quartet with an optimal separation achieved with Met_3, resulting in V_0 = 296.3 nM/s (Figure S15A). We also designed a parallel G4 with a 15-nucleotide single-stranded 3′ tail (Series VIII, Table 1): the tail can be hybridized with a complementary strand carrying a dC at its 3′ end (from 13- to 18-nucleotide long, Series IX, Table 1) in order to control the exact position of the dC relative to the quadruplex core. Again, we found that dC must be separated from the terminal G-quartet since the best results were obtained with the G4-T+15t system (V_0 = 183.7 nM/s, Figure S15B).

Potential Mechanism by which Adenine and Cytosine Proximal to the G4 Core Enhance DNAzyme Activity. To gain further mechanistic insights into G4-based biocatalysis, we performed a series of additional experiments. We first discarded differences in both hemin affinity for G4 and G4 stability as reasons for the dA/dC enhancements: neither hemin binding constants determined for the same panel of representative DNAzymes (Figures S16 and S17, K_d and K_a values are summarized in Table S2) nor the thermal stabilities of theses G4s (UV-melting experiments, Figure S18) correlated with Fe(III)-decay rate or DNAzyme activity. In other words, neither the hemin affinity nor the G4 stability were the limiting factors for DNAzyme activity. Then, we reevaluated our data in light of the nine-step catalytic cycle proposed in Figure 1: this mechanism is based on results that show a zero-order dependence of the catalysis on ABTS concentration and the linear kinetic relationship as a function of H_2O_2 concentration (Figure S19). These results indicated that the rate-determining step of the G4/hemin system is the

DOI: 10.1021/acscatal.8b03811
ACS Catal. 2018, 8, 11352−11361

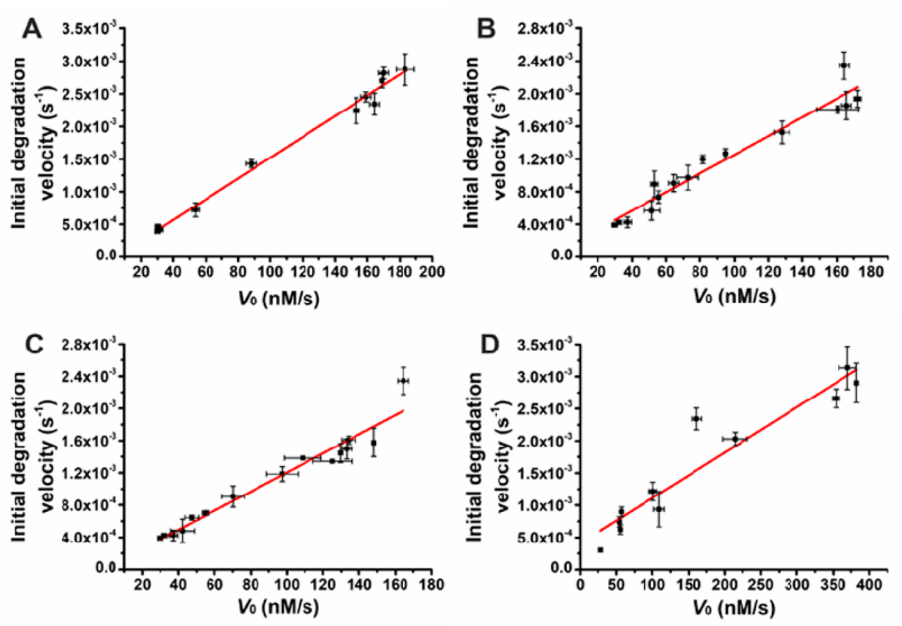

Figure 5. Linear correlation between the activity (V_0) and initial degradation velocity of G4/hemin in the presence of H_2O_2 with G4 bearing (A) dA in the second loop, (B) d[TC] near the 3′ end of the second loop, (C) d[CT] near the 5′ end of the second loop, and (D) dC in the flanking sequences. Note: the compared data were gathered from Figures 3 and 4.

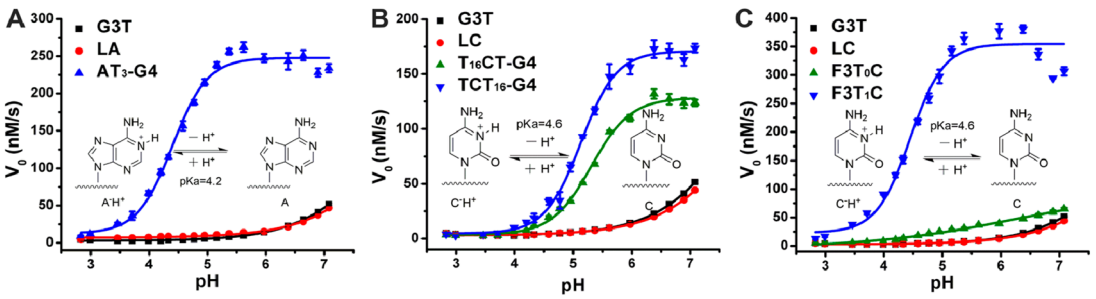

Figure 6. Plots of initial rates of G-quadruplex/hemin DNAzymes as a function of pH values with G4 bearing (A) dA in the loops, (B) dC in the loops, and (C) dC in the flanking sequences.

H_2O_2 binding to hemin to form the Compound 0 intermediate, which subsequently undergoes prototropic isomerization to produce Compound 0* and heterolytic cleavage of the O−O bond to lead to Compound 1, along with the loss of H_2O. We monitored the changes of the iron oxidation states (from Fe(III) (Compounds 0 and 0*) to Fe(IV) (Compound 1), Figure 1) via UV−vis spectra measurements performed with a representative panel of DNAzymes (Figure S20): before the addition of H_2O_2, all G4/hemin complexes showed absorbance signals at 500 and 630 nm, characteristic of a Fe(III) intermediates; the addition of H_2O_2 triggered a rapid (<2 min) decrease in the absorbance peak intensity and an increase of signals in the 550−620 and 650−700 nm regions, indicative of the formation of Compound 1. This correlation was further substantiated by a study of the Fe(III) decay rate (expressed as s^{-1}) as a function of the G4/hemin catalyst nature, in which the decay rates (Figures 4 and S21) were in perfect agreement with the activities (Figure 3) (that is, the fastest the Fe(III) consumption, the higher the catalytic rates, and their linear correlation were shown in Figure 5). These results demonstrated that the dA/dC enhancement is related to their capacity to accelerate the formation of Compound 1 within the corresponding G4/hemin system.

To gain further insight into the dA/dC roles, we turned our attention to the ionizable properties of dA/dC-modified G4s. In the native enzyme, His42 facilitates the transfer of H_2O_2 to the hemin iron atom. This transfer is made possible because the His42.H^+/His42 equilibrium has a pK_a of 2.5, compatible with that of hemin-bound H_2O_2/HO_2^- (pK_a between 3.2 and 4). A previous pK_a analysis performed with nucleoside triphosphates (ATP, CTP, GTP, and TTP) indicated that only ATP and CTP were compatible with this transfer (the pK_a values of ATP.H^+/ATP and CTP.H^+/CTP being 3.6 and 4.1 versus 9.8 for TTP/TTP^- and 2.2 and 9.5 for GTP.H^+/GTP/GTP^-).[34] To experimentally confirm that the ionization underlies the enhancement of DNAzyme activity by optimally placed dA or dC, we evaluated the catalytic properties of a representative panel of DNAzymes at pH values ranging from 2.83 to 7.08: our results (Figures 6 and S22) indicated that dA/dC-modified G4s (AT_3-, TCT_{16}-, T_{16}CT-G4, and F3T_1C) are markedly sensitive to pH (with an optimal activity at pH 5.0 and above), in stark contrast to the parent G4 (G3T) or DNAzymes with modifications located far from the hemin

DOI: 10.1021/acscatal.8b03811
ACS Catal. 2018, 8, 11352−11361

binding site (LA, LC, and F3T$_0$C, which display low activity and near pH insensitivity, Figure 6). The observation that low pH precluded dA/dC-mediated H_2O_2 proton transfer strongly supports the hypothesis according to which dA/dC mimic the role of a His42 in the native enzyme by accelerating Compound 1 formation.

DISCUSSION

Despite many reports describing activities of the G4-based biocatalysts, the synergistic action of the G4 core and the proximal nucleotides dA and/or dC to activate Compound 1 formation still remain to be uncovered. Here, we systematically varied the length and nature of G4 loops and flanking sequences, with the aim of gaining insights into the catalytically competent hemin binding site. We particularly focused on the spatial positioning of proximal dA or dC residues that may activate H_2O_2 prototropic cleavage in a manner that is reminiscent of the role played by His42 in the HRP active site. Interestingly, we observed that the dA/dC activating role was particularly significant with parallel-type G4s. This observation, combined with the wealth of data presented here, provides interesting clues on G4-based DNAzyme mechanism. The stability of the terminal G-quartet that serves as the hemin binding site depends on the overall G4 topology: previous investigations have shown that a guanine can flip out from the external G-quartet plane without disturbing the overall parallel G4 organization.[45,46] This observation is important since such flipped-out guanine may correspond to the "wobbling" guanine postulated by the Sen's group[47] to contribute to hemin activation. EPR[47] and UV−vis[48] data indicated that the iron atom of the G4-bound hemin is a hexacoordinated, high-spin species. This requires the presence of an axial ligand on the G4 side, which could be the wobbling guanine previously proposed (Figure S23), a free guanine that results from DNA strand slippage,[49] or an unidentified small molecule that binds between the G-quartet and the hemin. Although the exact nature of the sixth coordinating ligand remains to be discovered, our data demonstrate that the parallel G4 conformation and an optimally positioned dA/dC in the propeller loop or in the flanking region reconstitute the active site. Thus, we propose a new mechanistic step, schematically represented in Figure S23 that completes the proposed mechanism depicted in Figure 1 and provides a solid rationale for explaining the unique properties of G-quadruplex-based catalysts. Of course, further research will be necessary to experimentally confirm and refine the catalytic mechanism suggested in the present work. Our results also indicate that great care must be taken when positioning the H_2O_2-activating moieties because the exact position will strongly depend on the nature of the activator as demonstrated here with the difference between dA and dC, which originate in their purine versus pyrimidine nature with steric and electronic consequences.

CONCLUSIONS

Our data show that the proximal nucleobases dA/dC can mimic the role of histidine (His42) found in the active site of hemoproteins. The catalytic enhancement is efficient when dA/dC are inserted in both G-quadruplex loops and flanking regions, but a particular attention must be paid to the localization of the dA/dC enhancers. Our data allow us to refine the G4-based DNAzyme mechanism, highlighting how both G4 core and proximal nucleobases synergistically activate the Compound 0 → 0* prototropic cleavage of H_2O_2 to foster Compound 1 formation. Our results thus provide invaluable clues about the impact of G4-forming sequences on their overall catalytic competence and pave the way for further improvements that will ultimately make DNA-based catalysts fully competent with native enzymes.

ASSOCIATED CONTENT

Supporting Information

The Supporting Information is available free of charge on the ACS Publications website at DOI: 10.1021/acscatal.8b03811.

Additional tables and figures (PDF)

AUTHOR INFORMATION

Corresponding Authors

*E-mail for J.Z.: jun.zhou@nju.edu.cn. Tel.: +86-25-89683593. Fax: +86-25-89683593.
*E-mail for H.J.: hxju@nju.edu.cn.

ORCID

Jiri Šponer: 0000-0001-6558-6186
David Monchaud: 0000-0002-3056-9295
Jean-Louis Mergny: 0000-0003-3043-8401
Huangxian Ju: 0000-0002-6741-5302
Jun Zhou: 0000-0002-6793-3169

Notes

The authors declare no competing financial interest.

ACKNOWLEDGMENTS

This work was supported by the National Natural Science Foundation of China [21503229, 21635005, and 21361162002], Fundamental Research Funds for the Central Universities [020514380070, 020514380085, 020514380105, 020514380144 to J.Z.], self-funding projects from State Key Laboratory of Analytical Chemistry for Life Science, Nanjing University [5431ZZXM1711 to J.Z.], support from Nanjing University Innovation and Creative Program for PhD candidate [CXCY17-17 to J.C.], the Agence Nationale de la Recherche [ANR-17-CE17-0010-01], the European Research Council [H2020-MSCA-IF-2016-750368], the Université and Conseil Régional de Bourgogne (uB, CRB) and the European Union [PO FEDER-FSE Bourgogne 2014/2020 programs] [to D.M.], the Czech Science Foundation [GA16-13721S to J.S.], the ERDF project SYMBIT [CZ.02.1.01/0.0/0.0/15_003/0000477 to J.S. and J.L.M.]. J.L.M. is the recipient of the Recruitment Program for Foreign Experts (1000plan) of China [WQ20163200397] and funded by Nanjing University [020514912216].

REFERENCES

(1) Rawlings, N. D.; Barrett, A. J. Evolutionary Families of Peptidases. *Biochem. J.* **1993**, *290*, 205−218.
(2) Fedor, M. J.; Williamson, J. R. The Catalytic Diversity of RNAs. *Nat. Rev. Mol. Cell Biol.* **2005**, *6*, 399−412.
(3) Johnston, W. K.; Unrau, P. J.; Lawrence, M. S.; Glasner, M. E.; Bartel, D. P. RNA-Catalyzed RNA Polymerization: Accurate and General RNA-Templated Primer Extension. *Science* **2001**, *292*, 1319−1325.
(4) Liu, M.; Chang, D.; Li, Y. Discovery and Biosensing Applications of Diverse RNA-Cleaving DNAzymes. *Acc. Chem. Res.* **2017**, *50*, 2273−2283.

DOI: 10.1021/acscatal.8b03811
ACS Catal. 2018, 8, 11352−11361

(5) Taylor, A. I.; Pinheiro, V. B.; Smola, M. J.; Morgunov, A. S.; Peak-Chew, S.; Cozens, C.; Weeks, K. M.; Herdewijn, P.; Holliger, P. Catalysts from Synthetic Genetic Polymers. *Nature* **2015**, *518*, 427−430.
(6) Travascio, P.; Bennet, A. J.; Wang, D. Y.; Sen, D. A Ribozyme and a Catalytic DNA with Peroxidase Activity: Active Sites versus Cofactor-Binding Sites. *Chem. Biol.* **1999**, *6*, 779−787.
(7) Ponce-Salvatierra, A.; Wawrzyniak-Turek, K.; Steuerwald, U.; Höbartner, C.; Pena, V. Crystal Structure of a DNA Catalyst. *Nature* **2016**, *529*, 231−234.
(8) Schlosser, K.; Li, Y. Biologically Inspired Synthetic Enzymes Made from DNA. *Chem. Biol.* **2009**, *16*, 311−322.
(9) Breaker, R. R.; Joyce, G. F. A DNA Enzyme that Cleaves RNA. *Chem. Biol.* **1994**, *1*, 223−229.
(10) Coppins, R. L.; Silverman, S. K. A DNA Enzyme that Mimics the First Step of RNA Splicing. *Nat. Struct. Mol. Biol.* **2004**, *11*, 270−274.
(11) Sreedhara, A.; Li, Y.; Breaker, R. R. Ligating DNA with DNA. *J. Am. Chem. Soc.* **2004**, *126*, 3454−3460.
(12) Chinnapen, D. J. F.; Sen, D. A Deoxyribozyme that Harnesses Light to Repair Thymine Dimers in DNA. *Proc. Natl. Acad. Sci. U. S. A.* **2004**, *101*, 65−69.
(13) Barlev, A.; Sen, D. Catalytic DNAs that Harness Violet Light to Repair Thymine Dimers in a DNA Substrate. *J. Am. Chem. Soc.* **2013**, *135*, 2596−2603.
(14) Boersma, A. J.; Megens, R. P.; Feringa, B. L.; Roelfes, G. DNA-Based Asymmetric Catalysis. *Chem. Soc. Rev.* **2010**, *39*, 2083−2092.
(15) Megens, R. P.; Roelfes, G. DNA-Based Catalytic Enantioselective Intermolecular oxa-Michael Addition Reactions. *Chem. Commun.* **2012**, *48*, 6366−6368.
(16) Coquiere, D.; Feringa, B. L.; Roelfes, G. DNA-Based Catalytic Enantioselective Michael Reactions in Water. *Angew. Chem., Int. Ed.* **2007**, *46*, 9308−9311.
(17) Wang, J.; Benedetti, E.; Bethge, L.; Vonhoff, S.; Klussmann, S.; Vasseur, J. J.; Cossy, J.; Smietana, M.; Arseniyadis, S. DNA vs. Mirror-Image DNA: A Universal Approach to Tune the Absolute Configuration in DNA-Based Asymmetric Catalysis. *Angew. Chem., Int. Ed.* **2013**, *52*, 11546−11549.
(18) Chandra, M.; Silverman, S. K. DNA and RNA Can Be Equally Efficient Catalysts for Carbon-Carbon Bond Formation. *J. Am. Chem. Soc.* **2008**, *130*, 2936−2937.
(19) Roelfes, G.; Feringa, B. L. DNA-Based Asymmetric Catalysis. *Angew. Chem., Int. Ed.* **2005**, *44*, 3230−3232.
(20) Nakayama, S.; Sintim, H. Biomolecule Detection with Peroxidase-Mimicking DNAzymes; Expanding Detection Modality with Fluorogenic Compounds. *Mol. BioSyst.* **2009**, *6*, 95−97.
(21) Goertz, J. P.; White, I. M. Peroxidyme-Amplified Radical Chain Reaction (PARCR): Visible Detection of a Catalytic Reporter. *Angew. Chem., Int. Ed.* **2017**, *56*, 13411−13415.
(22) Sen, D.; Poon, L. C. RNA and DNA Complexes with Hemin [Fe (III) heme] are Efficient Peroxidases and Peroxygenases: How Do They Do It and What Does It Mean? *Crit. Rev. Biochem. Mol. Biol.* **2011**, *46*, 478−492.
(23) Poon, L. C. H.; Methot, S. P.; Morabi-Pazooki, W.; Pio, F.; Bennet, A. J.; Sen, D. Guanine-Rich RNAs and DNAs that Bind Heme Robustly Catalyze Oxygen Transfer Reactions. *J. Am. Chem. Soc.* **2011**, *133*, 1877−1884.
(24) Golub, E.; Albada, H. B.; Liao, W. C.; Biniuri, Y.; Willner, I. Nucleoapzymes: Hemin/G-Quadruplex DNAzyme-Aptamer Binding Site Conjugates with Superior Enzyme-like Catalytic Functions. *J. Am. Chem. Soc.* **2016**, *138*, 164−172.
(25) Poulos, T. L. Heme Enzyme Structure and Function. *Chem. Rev.* **2014**, *114*, 3919−3962.
(26) Chen, Q.; Liang, C.; Sun, X.; Chen, J.; Yang, Z.; Zhao, H.; Feng, L.; Liu, Z. H_2O_2-Responsive Liposomal Nanoprobe for Photoacoustic Inflammation Imaging and Tumor Theranostics via in Vivo Chromogenic Assay. *Proc. Natl. Acad. Sci. U. S. A.* **2017**, *114*, 5343−5348.
(27) Xiao, Y.; Pavlov, V.; Gill, R.; Bourenko, T.; Willner, I. Lighting Up Biochemiluminescence by the Surface Self-Assembly of DNA−Hemin Complexes. *ChemBioChem* **2004**, *5*, 374−379.
(28) Golub, E.; Freeman, R.; Willner, I. A Hemin/G-Quadruplex Acts as an NADH Oxidase and NADH Peroxidase Mimicking DNAzyme. *Angew. Chem., Int. Ed.* **2011**, *50*, 11710−11714.
(29) Albada, H. B.; Golub, E.; Willner, I. Rational Design of Supramolecular Hemin/G-quadruplex−Dopamine Aptamer Nucleoapzyme Systems with Superior Catalytic Performance. *Chem. Sci.* **2016**, *7*, 3092−3101.
(30) Nakayama, S.; Sintim, H. O. Investigating the Interactions between Cations, Peroxidation Substrates and G-Quadruplex Topology in DNAzyme Peroxidation Reactions Using Statistical Testing. *Anal. Chim. Acta* **2012**, *747*, 1−6.
(31) Golub, E.; Freeman, R.; Willner, I. Hemin/G-Quadruplex-Catalyzed Aerobic Oxidation of Thiols to Disulfides: Application of the Process for the Development of Sensors and Aptasensors and for Probing Acetylcholine Esterase Activity. *Anal. Chem.* **2013**, *85*, 12126−12133.
(32) Wang, Z. G.; Zhan, P.; Ding, B. Self-Assembled Catalytic DNA Nanostructures for Synthesis of Para-directed Polyaniline. *ACS Nano* **2013**, *7*, 1591−1598.
(33) Zhu, L.; Li, C.; Zhu, Z.; Liu, D.; Zou, Y.; Wang, C.; Fu, H.; Yang, C. J. In Vitro Selection of Highly Efficient G-Quadruplex-Based DNAzymes. *Anal. Chem.* **2012**, *84*, 8383−8390.
(34) Stefan, L.; Denat, F.; Monchaud, D. Insights into How Nucleotide Supplements Enhance the Peroxidase-Mimicking DNAzyme Activity of the G-Quadruplex/Hemin System. *Nucleic Acids Res.* **2012**, *40*, 8759−8772.
(35) Kong, D. M.; Xu, J.; Shen, H. X. Positive Effects of ATP on G-Quadruplex-Hemin DNAzyme-Mediated Reactions. *Anal. Chem.* **2010**, *82*, 6148−6153.
(36) Stefan, L.; Denat, F.; Monchaud, D. Deciphering the DNAzyme Activity of Multimeric Quadruplexes: Insights into Their Actual Role in the Telomerase Activity Evaluation Assay. *J. Am. Chem. Soc.* **2011**, *133*, 20405−20415.
(37) Qi, C.; Zhang, N.; Yan, J.; Liu, X.; Bing, T.; Mei, H.; Shangguan, D. Activity Enhancement of G-Quadruplex/Hemin DNAzyme by Spermine. *RSC Adv.* **2014**, *4*, 1441−1448.
(38) Chen, J.; Guo, Y.; Zhou, J.; Ju, H. The Effect of Adenine Repeats on G-Quadruplex/Hemin Peroxidase Mimicking DNAzyme Activity. *Chem. - Eur. J.* **2017**, *23*, 4210−4215.
(39) Li, W.; Li, Y.; Liu, Z.; Lin, B.; Yi, H.; Xu, F.; Nie, Z.; Yao, S. Insight into G-quadruplex-Hemin DNAzyme/RNAzyme: Adjacent Adenine as the Intramolecular Species for Remarkable Enhancement of Enzymatic Activity. *Nucleic Acids Res.* **2016**, *44*, 7373−7384.
(40) Chang, T.; Gong, H.; Ding, P.; Liu, X.; Li, W.; Bing, T.; Cao, Z.; Shangguan, D. Activity Enhancement of G-Quadruplex/Hemin DNAzyme by Flanking d (CCC). *Chem. - Eur. J.* **2016**, *22*, 4015−4021.
(41) Jones, P.; Dunford, H. B. The Mechanism of Compound I Formation Revisited. *J. Inorg. Biochem.* **2005**, *99*, 2292−2298.
(42) Del Villar-Guerra, R.; Trent, J. O.; Chaires, J. B. G-Quadruplex Secondary Structure Obtained from Circular Dichroism Spectroscopy. *Angew. Chem., Int. Ed.* **2018**, *57*, 7171−7175.
(43) Nakayama, S.; Wang, J.; Sintim, H. O. DNA-Based Peroxidation Catalyst—What Is the Exact Role of Topology on Catalysis and Is There a Special Binding Site for Catalysis? *Chem. - Eur. J.* **2011**, *17*, 5691−5698.
(44) Guédin, A.; Gros, J.; Alberti, P.; Mergny, J. L. How Long Is too Long? Effects of Loop Size on G-Quadruplex Stability. *Nucleic Acids Res.* **2010**, *38*, 7858−7868.
(45) Ourliac-Garnier, I.; Elizondo-Riojas, M. A.; Redon, S.; Farrell, N. P.; Bombard, S. Cross-Links of Quadruplex Structures from Human Telomeric DNA by Dinuclear Platinum Complexes Show the Flexibility of Both Structures. *Biochemistry* **2005**, *44*, 10620−10634.
(46) Bertrand, H.; Bombard, S.; Monchaud, D.; Teulade-Fichou, M. P. A Platinum-Quinacridine Hybrid as a G-Quadruplex Ligand. *J. Biol. Inorg. Chem.* **2007**, *12*, 1003−1014.

DOI: 10.1021/acscatal.8b03811
ACS Catal. 2018, 8, 11352−11361

(47) Travascio, P.; Witting, P. K.; Mauk, A. G.; Sen, D. The Peroxidase Activity of a Hemin-DNA Oligonucleotide Complex: Free Radical Damage to Specific Guanine Bases of the DNA. *J. Am. Chem. Soc.* **2001**, *123*, 1337−1348.
(48) Travascio, P.; Li, Y.; Sen, D. DNA-Enhanced Peroxidase Activity of a DNA Aptamer-Hemin Complex. *Chem. Biol.* **1998**, *5*, 505−517.
(49) Stadlbauer, P.; Krepl, M.; Cheatham, T. E.; Koča, J.; Šponer, J. Structural Dynamics of Possible Late-Stage Intermediates in Folding of Quadruplex DNA Studied by Molecular Simulations. *Nucleic Acids Res.* **2013**, *41*, 7128−7143.

NOTE ADDED AFTER ASAP PUBLICATION

The version of this paper that was published ASAP November 2, 2018, contained an error in the pagination and layout of the Supporting Information. The corrected version was reposted November 5, 2018.

DOI: 10.1021/acscatal.8b03811
ACS Catal. 2018, 8, 11352−11361